HANDBOOK OF NANOPHYSICS

Principles and Methods

Edited by

Klaus D. Sattler

Nanomechanical Properties of the Elements

Nicola M. Pugno
Politecnico di Torino

23.1 Introduction

Recently, the interest on the mechanical properties of materials at the nanoscale level has been remarkably growing. Just in the last few decades, material scientists have been able to make direct measurements at such a critical size scale, three orders of magnitude smaller than the more known and accessible microscale. An example is given by the exceptional mechanical properties observed in nanotubes (Ross, 1991; Treacy et al., 1996; Yakobson et al., 1996, 1997; Yakobson and Smalley, 1997) since their re-discovery (see Pugno 2008) by Sumio Iijima (1991) and other scientists (Chopra et al., 1995; Weng-Sieh et al., 1995; Loiseau et al., 1996). The tremendous mechanical properties coupled with the exceptional electronic ones lead to consider nanoscale materials as optimal candidates for innovative materials (e.g., bio-inspired), for biomechanical applications (e.g., nanorobots), or electronics (e.g., nanoelectromechanical systems) (see the review by Qian et al. 2002).

Following the increasing interest in nanomechanics, this chapter intends to review the new results reported in the study of the mechanical properties of materials at the nanoscale (Pugno et al. 2006). We have shown that only two parameters are needed to describe the nanomechanics of materials: the cohesion energy and the atomic size. The proposed simple but general model gives, as a result, a preliminary periodic table for the nanomechanical properties of elements in which a periodicity of the mechanical properties emerges. As a simple example of application for

the reader, the theory is applied to the very recent results on the measurement of the elastic properties and intrinsic strength of monolayer graphene (Lee et al., 2008).

23.2 Nonlinear Normal Stress–Strain Law

Let us consider—for the sake of simplicity—a material arranged in the simple cubic lattice with lattice spacing a. Around the equilibrium position, linear elasticity is expected whereas for larger displacements, a nonlinearity takes place. As we will show, the nonlinearity in the constitutive equation has to be considered for developing a general model including the effect of the coefficient of thermal expansion.

Anisotropy is not taken into account in our model, the aim of which is to give simple estimations of the nanomechanical properties of materials. However, different types of lattices could be treated by considering as a first approximation an equivalent simple cubic lattice (e.g., by equating the atomic volumes).

The interatomic potential U between atoms depends substantially on their chemical bonding. The atoms do not come into contact owing to Pauli's and nuclei repulsions and reach their equilibrium positions. Even if different chemical bonds imply different interatomic potentials (e.g., Lennard-Jones), we can consider a general form (representing the interaction between one atom and all the others) according to the following series expansion:

$$U(x) = \sum_{n=0}^{N} c_n x^n, \qquad (23.1)$$

where

x is the displacement around the equilibrium position
c_n are unknown coefficients
N is the order of the polynomial approximation

The force F between atoms will be

$$F(x) = \frac{dU(x)}{dx}. \qquad (23.2)$$

We can assume $c_0 = 0$, the energy being defined through its differential, and we must have $c_1 = 0$, the net force being vanishing at the equilibrium point $x = 0$. The classical harmonic approximation sets $N = 2$ and gives a linear relationship between force and displacement, the so-called Hooke's law. In addition, this symmetric form for the potential energy, related to small displacements, predicts vanishing thermal expansion, in contrast to the experimental evidence. Thus, at least an additional term has to be assumed so that a value of $N = 3$ is here considered. According to the simplified hypothesis of isotropic regular lattice, a volume $a \times a \times a$ per each atom is considered (simple cubic lattice). The two unknown constants c_2 and c_3 can be obtained by imposing the definitions of Young's modulus and coefficient of thermal expansion, i.e.,

$$\lim_{x \to 0} \frac{F(x)}{xa} = E, \qquad (23.3a)$$

$$\frac{\langle x \rangle}{aT} = \alpha, \qquad (23.3b)$$

$\langle x \rangle$ being the mean value of the displacement due to the thermal vibration at temperature T. The first condition implies $c_2 = Ea/2$. On the other hand, the second one, evaluating $\langle x \rangle$ by means of the Boltzmann's distribution, i.e.,

$$\langle x \rangle = \frac{\int_{-\infty}^{+\infty} x e^{-\beta U(x)} dx}{\int_{-\infty}^{+\infty} e^{-\beta U(x)} dx} \approx \frac{\int_{-\infty}^{+\infty} x e^{-\beta c_2 x^2}(1 - \beta c_3 x^3) dx}{\int_{-\infty}^{+\infty} e^{-\beta c_2 x^2} dx}, \quad (23.4)$$

where

$\beta = (k_B T)^{-1}$
k_B is Boltzmann's constant, gives $c_3 = -E^2 a^3 \alpha/(3k_B)$

In terms of local stress $\sigma = F/a^2$ and strain $\varepsilon = x/a$, the result is

$$\sigma(\varepsilon) \approx E\varepsilon - \frac{E^2 a^3 \alpha}{k_B} \varepsilon^2, \quad \text{for } \varepsilon \leq \varepsilon_C. \qquad (23.5)$$

Even if the considered approach, based on the interatomic potential, is very simple (Kittel, 1966), the result of Equation 23.5 is original and describes a general form for the stress–strain relationship at nanoscale: for small displacements, it recovers the
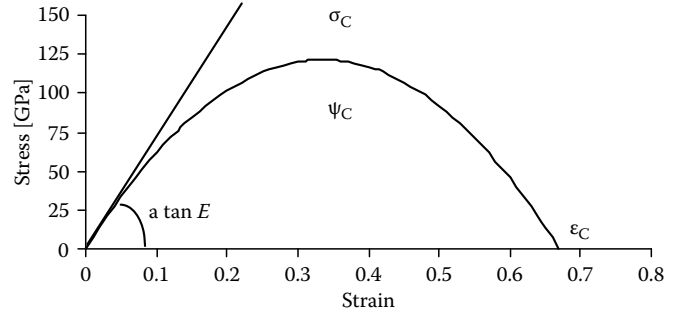
FIGURE 23.1 Nano-stress vs. nano-strain relationship (for carbon). Young's modulus E, critical stress σ_C and strain ε_C and energy density (or fragmentation energy) ψ_C. (From Pugno, N. et al., *Int. J. Solids Struct.*, 43, 5647, 2006. With permission.)

well-known Hooke's law, whereas for large displacements, a non-Hookean softening regime dominates. Note that the multibody nature of the atomic interaction is automatically taken into account in Equation 23.5 via Young's modulus. However, more sophisticated multibody potential could be easily considered (Zhang et al., 2002). The cutoff at ε_C is analogous to those classically introduced in the interatomic potentials. This is imposed by the fact that, after the critical (i.e., maximum) strain ε_C for which the stress vanishes, the approximation of Equation 23.5 loses its validity. Equation 23.5 is general in the sense that the atomic (or electronic or chemical bonding) structure of the solid is traduced in terms of global parameters.

According to Equation 23.5, the critical (i.e., maximum) stress and strain are predicted to be

$$\sigma_C \approx \frac{k_B}{4\alpha a^3}, \qquad (23.6a)$$

$$\varepsilon_C \approx \frac{k_B}{E\alpha a^3}. \qquad (23.6b)$$

Note that ε_C represents the maximum strain assuming a displacement-controlled process. Vice-versa, for a force-controlled process, the critical strain is one-half of the previous one and will be reached at the maximum stress (see Figure 23.1).

23.3 Cohesion Energies

The energy dissipated per unit volume a^3, that we could call fragmentation energy (Carpinteri and Pugno, 2002), can be calculated starting from the nonlinear relationship of Equation 23.5 as

$$\Psi_C \approx \int_0^{\varepsilon_C} \sigma(\varepsilon) d\varepsilon \approx \frac{k_B^2}{6Ea^6 \alpha^2}. \qquad (23.7)$$

Thus, the energy dissipated per unit area a^2, the so-called fracture energy (Carpinteri, 1997), is

$$G_C \approx \Psi_C a \approx \frac{k_B^2}{6Ea^5 \alpha^2}. \qquad (23.8)$$

The fracture energy plays a fundamental role in the prediction of the resistance against brittle crack propagation for a structural element (Pugno and Carpinteri, 2003).

On the other hand, the energy to pull-out an atom from the lattice, the so-called cohesion energy (Kittel, 1966), must be equal to

$$W_C \approx G_C 6a^2 \approx \frac{k_B^{\ 2}}{Ea^3\alpha^2}, \qquad (23.9)$$

where $6a^2$ is the new surface area created after the pull-out of one atom from the lattice, according to our simplified model.

23.4 Young's Modulus and Coefficient of Thermal Expansion Correlation

Young's modulus is an index of the stiffness of a material against mechanical loadings, whereas the coefficient of thermal expansion is an index of the compliance of a material under thermal variations. The aim of this section is to find, by virtue of a simplified argument, their correlation.

Let us consider the differential of the free energy u, given by (Kittel, 1966) $du = -p\,dV - S\,dT$, where the pressure p and the entropy S are defined as $p = -(\partial u/\partial V)_T$, $S = -(\partial u/\partial T)_V$, and V is the volume. At the thermodynamical equilibrium, $du = 0$, so that $p = -S(dT/dV) = (\partial u/\partial T)_V(dT/dV)$. For one atom, the contribution to the free energy due to the thermal vibrations can be classically considered equal to $\sim 3/2 k_B T$. Assuming constant pressure, the coefficient of thermal expansion being defined as $\alpha = (3V)^{-1}\,dV/dT$, the previous relationship would give $p = k_B/(2V\alpha)$. On the other hand, assuming constant temperature, differentiating and introducing the stress σ and strain ε under hydrostatic pressure p, for one atom of volume $V \approx a^3$, we have

$$dp = -d\sigma = -\frac{k_B}{2\alpha}\frac{dV}{V^2} = -\frac{k_B}{2\alpha a^3}3d\varepsilon. \qquad (23.10)$$

Isotropic linear elastic constitutive laws (see Carpinteri, 1997) are expected for small strains, implying, under hydrostatic regime, the following relationship:

$$\frac{d\sigma}{d\varepsilon} = \frac{E}{1-2\nu}, \qquad (23.11)$$

where ν is the Poisson's ratio of the material. The combination of the two previous equations provides the following correlation between Young's modulus and coefficient of thermal expansion as

$$E \approx \frac{3k_B(1-2\nu)}{2\alpha a^3}. \qquad (23.12)$$

As expected, they are inversely related. This result coincides with Grüneisen's relation evaluated for one atom, in which the

thermal capacity is assumed to be equal to $3k_B$ (the classical value around room temperature) and Grüneisen's experimental constant is assumed to be equal to 3/2, close to its experimental value for many chemical elements (Slater, 1940). However, note that the thermal expansion coefficient and Young's modulus are functions of temperature (Jiang et al., 2004).

23.5 Nonlinear Shear Stress–Strain Law

In Equation 23.12 a new elastic constant appears, i.e., the Poisson's ratio ν that, with Young's modulus E, allows one to describe the elastic properties of isotropic materials. What is the expected value for ν at the nanoscale? To evaluate this coefficient, that thermodynamically must be comprised between -1 and $1/2$, we can alternatively evaluate the shear elastic modulus G.

For small displacements, the shear stress τ is connected with the displacement y (perpendicular to the previously introduced x coordinate) by Hooke's law, i.e.,

$$\tau = G\frac{y}{a}. \qquad (23.13)$$

Due to the periodicity of the lattice with respect to shear, the relation shear stress vs. displacement can be assumed as (Frenkel, 1926):

$$\tau \approx \frac{G}{2\pi}\sin\left(2\pi\frac{y}{a}\right), \qquad (23.14)$$

showing a non-Hookean region for large displacements. Obviously, for small displacements it becomes Hooke's law of Equation 23.13. As a consequence, the maximum value of the shear stress is

$$\tau_C \approx \frac{G}{2\pi}. \qquad (23.15)$$

The ideal shear strength is predicted to be approximately only one order of magnitude smaller than the shear elastic modulus (Frenkel, l926). Even if the correct coefficient of proportionality remains unknown, depending on the adopted model, this result is experimentally verified and represents an interesting tool to discriminate if the measurements on material strength are close or not to the ideal material strength. The simple approach reported in Section 23.2 can be considered the extension of this approach for the normal stress–strain relationship.

The shear strain γ is defined by $\tan\gamma = y/a$, so that the nonlinear shear stress vs. strain relationship at the nanoscale is predicted as

$$\tau \approx \frac{G}{2\pi}\sin(2\pi\tan\gamma). \qquad (23.16)$$

The critical value of the shear strain γ will be reached, in a displacement-controlled process, when the shear stress vanishes, for

$$\gamma_C = a\tan 1/2 \approx 27°. \tag{23.17}$$

On the other hand, if the process is force-controlled, then the critical value of the shear strain will be reached when the stress equals its critical value. The corresponding shear strain level is atan1/4 ≈ 14°. This parameter is very large if compared with the measured values at human size scale (of the order of the meter). In addition, it is material-independent. This means that, at nanoscale, the ductility—which is not a material property but a size-dependent parameter—seems to "universally" prevail over brittleness, independently of the considered material.

Considering the derived strength of Equation 23.6a, and replacing α by Equation 23.12, gives $\sigma_C \approx E/(6(1-\nu))$. Thus, the model confirms that the ideal strength is expected as a significant fraction of Young's modulus: such result can be considered a proof of consistency for the simple model that we are proposing. Assuming the well-known tensional Tresca's or energetic von Mises' criteria (usually considered in plasticity but still applicable if a brittle collapse is assumed, see Carpinteri, 1997)

$$\sigma_C \approx \lambda_{T,vM}\tau_C, \tag{23.18}$$

where $\lambda_T = 2$ or $\lambda_{vM} = \sqrt{3}$ for the two criteria respectively. By comparison between the normal and shear strengths, noting that $G = E/(2(1+\nu))$, we deduce an estimation of the Poisson's ratio at the nanoscale as

$$\nu \approx \frac{3\lambda_{T,vM} - 2\pi}{6\lambda_{T,vM} + 2\pi} \approx 0. \tag{23.19}$$

According to Tresca's criterion, the prediction is of $\nu_T = -0.015$, as well as for von Mises' criterion of $\nu_{vM} = -0.065$. Practically, both criteria suggest Poisson's ratio close to zero. A prediction of ν outside its thermodynamical domain [−1, 1/2] would show an inconsistency of our model. On the contrary and in spite of its simplicity, it appears to be *self-consistent*. Obviously, the prediction of Poisson's ratio close to zero has to be taken with caution, representing only an estimation of our simplified model. However, a surprisingly close to zero Poisson's ratio of $\nu \approx 0.07$ has been measured for nanotubes by means of Brillouin light scattering (Casari et al., 2001).

23.6 Nanomechanical Properties of the Elements

Eliminating the coefficient of thermal expansion in the derived nanomechanical properties, and assuming a Poisson's ratio equal to zero, gives the following estimation for the nanomechanical properties as a function of the cohesion energy W_C and of the atomic size a:

$$G_C \approx \frac{W_C}{6a^2}, \quad \Psi_C \approx \frac{G_C}{a}, \tag{23.20a}$$

$$\nu \approx 0, \quad E \approx \frac{27}{2}\Psi_C, \tag{23.20b}$$

$$\sigma_C \approx \frac{E}{6}, \quad \tau_C \approx \frac{E}{4\pi}, \tag{23.20c}$$

$$\varepsilon_C \approx \frac{2}{3}, \quad \gamma_C \approx a\tan\frac{1}{2}. \tag{23.20d}$$

Better estimations could be deduced relaxing the simplified hypothesis of ν ≈ 0. Note the large critical normal and shear strains suggest large ductility at the nanoscale, independently from the considered material. Such a result seems to be confirmed by the large ductility shown by classically brittle materials (if considered at the human size scale) like glass or carbon, e.g., glass whiskers or carbon nanotubes (Yakobson et al., 1997).

23.7 Comparison with the Literature

The most well-known prediction for the ideal strength of crystals was derived by Orowan (1948) in the following form:

$$\sigma_C^{(Orowan)} \approx \sqrt{\frac{EG_C}{2a}} \tag{23.21}$$

A detailed comparison between the Orowan's prediction and a large number of experimental observations was reported by Macmillan (1983), demonstrating that, in spite of its simplicity, Equation 23.21 can reasonably predict the ideal strength of materials. Thus, if our approach agrees with such a prediction, we conclude that it has to be considered in agreement with the experimental observations on ideal strength of solids. Obviously, our approach as well as the Orowan's estimation have to be considered as reasonable estimations rather than as exact predictions. Rearranging Equations 23.20 we find

$$\sigma_C \approx \sqrt{\frac{27}{36}}\sqrt{\frac{EG_C}{2a}} \approx 0.9\sigma_C^{(Orowan)}. \tag{23.22}$$

Thus, the two estimations are in reciprocal agreement.

Finally, we note that, applying quantized fracture mechanics (Pugno and Ruoff, 2004) considering the fracture quantum as coincident with the atomic size, the prediction of the ideal strength is

$$\sigma_C^{(QFM)} \approx \sqrt{\frac{4}{\pi}}\sqrt{\frac{EG_C}{2a}} \approx 1.1\sigma_C^{(Orowan)}, \tag{23.23}$$

again in agreement with the previous model.

Now, let us focus the attention on carbon (graphitic form), for which $a \approx 1.54$ Å and $W_C \approx 7.36$ eV/atom (Kittel, 1966). Correspondingly, from Equations 23.20, we estimate the following:

1. ν ≈ 0; experiments on carbon nanotubes seem to confirm this prediction: a surprisingly close to zero value of ν ≈ 0.07 has been measured (Casari et al., 2001).
2. $E \approx 725$ GPa; it is well-known that Young's modulus for ideal carbon nanotubes, or graphite, is expected to be of

the order of $E \approx 1\,\text{TPa}$ (Qian et al., 2002). Values close to 800 GPa were measured by Yu et al. (2000).

3. $G_C \approx 8.3\,\text{N/m}$ (and $\Psi_C \approx 54\,\text{GPa}$); a reference value for carbon nanotubes is $G_C \approx 8.4\,\text{N/m}$ (Lambin et. al., 1998).

4. $\varepsilon_C \approx 67\%$ (and $\gamma_C \approx 27°$); based on molecular dynamics atomistic simulations (Yakobson et al., 1997), a value of $\varepsilon_C \approx 40\%$ is locally predicted in monoatomic chains due to high strain fracture of carbon nanotubes.

5. $\sigma_C \approx 121\,\text{GPa}$ (and $\tau_C \approx 58\,\text{GPa}$); strength of ideal carbon nanotubes, or graphite, is expected to be of the order of $\sigma_C \approx 100\,\text{GPa}$ (Qian et al., 2002). Values up to 64 GPa were measured by Yu et al. (2000).

Eventually, the toughness at the nanoscale is predicted by definition as $K_{IC} = \sqrt{G_C E} \approx 2.45\,\text{MPa}\sqrt{\text{m}}$, and, from Equation 23.12, the coefficient of thermal expansion is $\alpha \approx 8 \times 10^{-6}\,\text{K}^{-1}$.

The nanoscale stress–strain relationship of carbon, Equation 23.5, is reported in Figure 23.1.

It is important to note that the predicted values substantially agree with the experimental results at the nanoscale and that they are completely different from the corresponding values at the macroscale. In fact, strong size effects on material properties are expected (Carpinteri and Pugno, 2004).

23.8 Nanomechanics Is the Borderline between Classical and Quantum Mechanics

The last considerations are on brittle crack propagation at the nanoscale. The velocity of the crack propagation, as well as of the elastic waves, is of the order of $\sqrt{E/\rho}$, ρ being the density of the considered material. According to special relativity, it must be smaller than light velocity c, so that the corresponding maximum value of Young's modulus results to be $E_{SR_{max}} \approx \rho c^2$, and therefore around $10^{20}\,\text{Pa}$ for $\rho \approx 10^3\,\text{kg/m}^3$ (thus, much larger than the observed values).

A more interesting upper-bound for Young's modulus is imposed by quantum mechanics, considering fracture propagation at the nanoscale coupled with the Heisenberg's principle. In one of its forms, the principle states that $\Delta W\,\Delta t \geq \hbar$, where ΔW and Δt are, respectively, the energy and the time spent in the process, and $\hbar = h/2\pi$, where h is the Planck's constant. With reference to fracture propagation, evaluating the time as $\Delta t \approx a/\sqrt{E/\rho}$, and the energy as $\Delta W \approx G_C a^2$, we obtain

$$E_{QM_{max}} \approx \frac{\rho G_C^2 a^6}{\hbar^2}, \tag{23.24}$$

which, for $\rho \approx 10^3\,\text{kg/m}^3$, $G_C \approx 10\,\text{N/m}$, and $a \approx 1\,\text{Å}$, is found to be around 10 TPa and of the same order of magnitude (TPa) observed for example in carbon nanotubes. This very simple argument is intended to show that nanomechanics can be considered at the borderline between classical and quantum mechanics (and, obviously, outside the domain of special relativity). This is the

reason why both classical and quantum mechanics have been successfully applied in nanomechanical treatments.

23.9 Periodic Table for the Nanomechanical Properties of Elements

According to Equations 23.22, and based on the values of the interatomic distances in the stable lattice reported (Table of Periodic Properties of The Elements by Sargent-Scientific Laboratory Equipment Catalog Number S18806) and of the cohesion energies (Kittel, 1966; referred to 0 K), the nanomechanical properties of the elements (for which both the interatomic distance and cohesion energy are known) as functions of their atomic number are depicted in Figures 23.2 through 23.8.

FIGURE 23.2 Nano-fracture energy G_C of elements vs. atomic number. (From Pugno, N. et al., *Int. J. Solids Struct.*, 43, 5647, 2006. With permission.)

FIGURE 23.3 Nano-fragmentation energy ψ_C of elements vs. atomic number. (From Pugno, N. et al., *Int. J. Solids Struct.*, 43, 5647, 2006. With permission.)

FIGURE 23.4 Nano-Young's modulus E of elements vs. atomic number. (From Pugno, N. et al., *Int. J. Solids Struct.*, 43, 5647, 2006. With permission.)

FIGURE 23.5 Nano-normal strength σ_C of elements vs. atomic number. (From Pugno, N. et al., *Int. J. Solids Struct.*, 43, 5647, 2006. With permission.)

FIGURE 23.6 Nano-shear strength τ_C of elements vs. atomic number. (From Pugno, N. et al., *Int. J. Solids Struct.*, 43, 5647, 2006. With permission.)
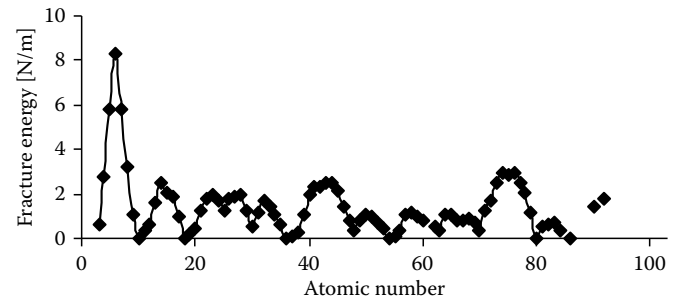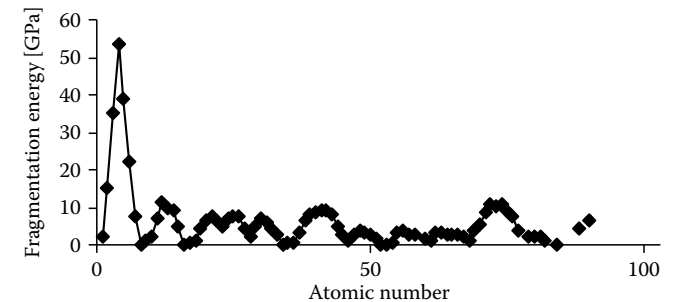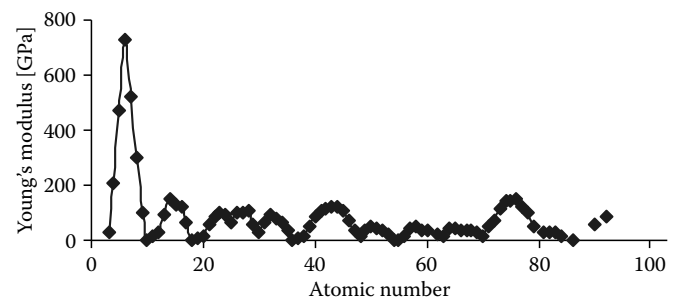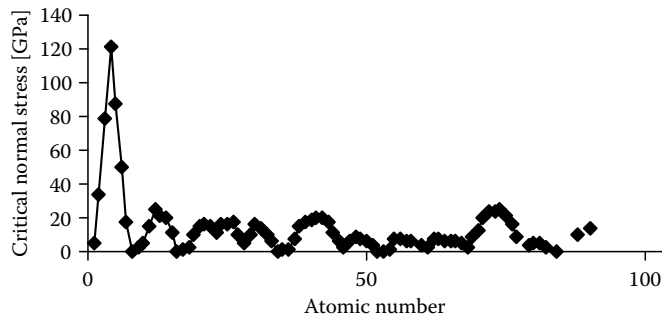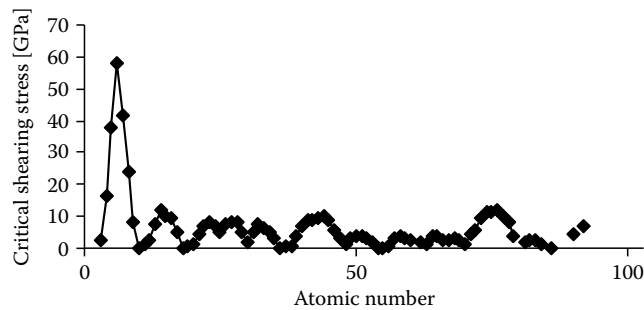

FIGURE 23.7 Nano-fracture toughness K_{IC} of elements vs. atomic number. (From Pugno, N. et al., *Int. J. Solids Struct.*, 43, 5647, 2006. With permission.)

FIGURE 23.8 Inverse of the coefficient of thermal expansion α of elements vs. atomic number. (From Pugno, N. et al., *Int. J. Solids Struct.*, 43, 5647, 2006. With permission.)
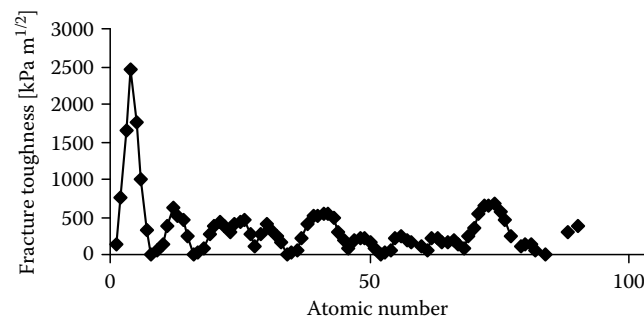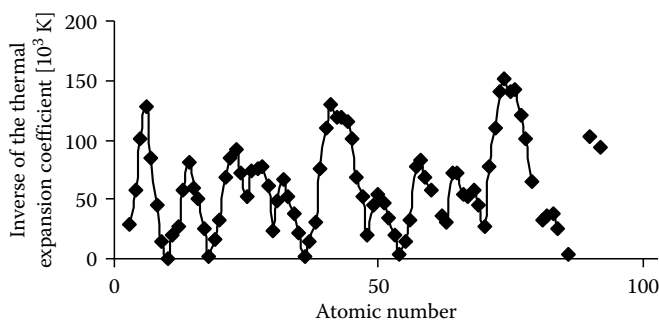
A preliminary periodic table for the nanomechanical properties of elements is reported in Table 23.1. We have focused our attention on the main mechanical properties of materials, i.e., Young's modulus, the strength, and the fracture toughness. The periodicity in the nanomechanical properties appears in a very clear way. Carbon—the chemical foundation of life—appears to be the strongest element.

23.10 Example of Application: Nonlinear Elasticity and Strength of Graphene

An explosion of interest in the fabrication and characterization of graphene sheets is currently taking place (Novoselov et al., 2004; Berger et al., 2006; Stankovich et al., 2006; Dikin et al., 2007) due to their predicted fascinating mechanical (and electrical) properties and thanks to recently available new nanotechnological tools. In the paper by Lee et al. (2008), the authors measured, by atomic force nanoindentation, the elastic properties and the ideal strength of free-standing monolayer graphene sheets.

The material constitutive law was assumed to be isotropic nonlinear elastic, in the form of $\sigma = E\varepsilon + D\varepsilon^2$, where σ is the stress, ε is the strain, E is Young's modulus, and D is the third-order elastic modulus. They measured values of $E = 1.0 \pm 0.1$ TPa and $D = -2.0 \pm 0.4$ TPa. While a one terapascal Young's modulus was expected and consistent with the abundant data in the literature, the measurement of D reveals new insights regarding the nonlinear elastic behavior of graphene. In order to check the plausibility of their computed value, we may note that our model predicts $D = -E^2 a^3 \alpha / k_B$, where α is the (linear) expansion coefficient, k_B is the Boltzmann's constant, and a is here the C–C bond length (in graphene). Thus, we could indirectly estimate the thermal expansion coefficient of the tested monolayer graphene membranes, plausibly finding $\alpha \approx 1.0 \times 10^{-5}$ K^{-1}, which suggests the consistence of the reported third-order elastic modulus (or, vice versa, assuming $\alpha \approx 1.0 \times 10^{-5}$ K^{-1} one would deduce $D \approx -2.1$ TPa).

The nonlinear elasticity affected only the small region of the graphene around the point where the load was applied and not the cubic force–load displacement curve (as imposed by the large displacements involved in the stretching). Accordingly, under the atomic force tip, a stress/strain concentration took place, numerically computed by the authors (Lee et al., 2008), from which the material strength was derived. Even if the precision of an intrinsic strength measurement based on the stress–concentration concept of the continuum (which ignores energy release rate and quantization) is questionable, leading toward stress-intensifications to obvious strength overestimations, a value of $\sigma_{int} = 130 \pm 10$ GPa was deduced following a rigorous approach. The predicted huge strength suggests to have measured the ideal material intrinsic strength, expected to be of the order of one tenth of Young's modulus. Weibull moduli, one order of magnitude larger than those that we observed in carbon nanotubes, showed a more deterministic failure and seem

TABLE 23.1 Periodic Table for the Nanomechanical Properties of the Elements

$^{1}\mathrm{H}$	The Periodic Table for the Nanomechanical Properties of the Elements																$^{2}\mathrm{He}$
$_{31}^{3}\mathrm{Li}_{137}^{5}$	$_{206}^{4}\mathrm{Be}_{751}^{34}$			$_{E[GPa]=725}^{Z=6}\mathrm{C}_{2450=K_{IC}[kPa\sqrt{m}]}^{121=\sigma_C[GPa]}$								$_{474}^{5}\mathrm{B}_{1653}^{79}$	$_{725}^{6}\mathrm{C}_{2450}^{121}$	$_{525}^{7}\mathrm{N}_{1749}^{87}$	$_{301}^{8}\mathrm{O}_{989}^{50}$	$_{101}^{9}\mathrm{F}_{331}^{17}$	$_{0.4}^{10}\mathrm{Ne}_{1.8}^{0.07}$
$_{14}^{11}\mathrm{Na}_{67}^{2}$	$_{31}^{12}\mathrm{Mg}_{138}^{5}$											$_{91}^{13}\mathrm{Al}_{382}^{15}$	$_{153}^{14}\mathrm{Si}_{619}^{25}$	$_{130}^{15}\mathrm{P}_{514}^{22}$	$_{121}^{16}\mathrm{S}_{471}^{20}$	$_{65}^{17}\mathrm{Cl}_{249}^{11}$	$_{0.7}^{18}\mathrm{Ar}_{3.5}^{0.1}$
$_{6}^{19}\mathrm{K}_{30}^{1}$	$_{16}^{20}\mathrm{Ca}_{79}^{3}$	$_{59}^{21}\mathrm{Sc}_{274}^{10}$	$_{87}^{22}\mathrm{Ti}_{390}^{14}$	$_{99}^{23}\mathrm{V}_{442}^{17}$	$_{90}^{24}\mathrm{Cr}_{391}^{15}$	$_{67}^{25}\mathrm{Mn}_{290}^{11}$	$_{97}^{26}\mathrm{Fe}_{417}^{16}$	$_{101}^{27}\mathrm{Co}_{435}^{17}$	$_{105}^{28}\mathrm{Ni}_{449}^{17}$	$_{60}^{29}\mathrm{Cu}_{271}^{10}$	$_{27}^{30}\mathrm{Zn}_{119}^{5}$	$_{63}^{31}\mathrm{Ga}_{270}^{10}$	$_{96}^{32}\mathrm{Ge}_{408}^{16}$	$_{80}^{33}\mathrm{As}_{336}^{13}$	$_{61}^{34}\mathrm{Se}_{255}^{10}$	$_{37}^{35}\mathrm{Br}_{152}^{6}$	$_{0.8}^{36}\mathrm{Kr}_{4.1}^{0.1}$
$_{4}^{37}\mathrm{Rb}_{23}^{1}$	$_{11}^{38}\mathrm{Sr}_{58}^{2}$	$_{46}^{39}\mathrm{Y}_{227}^{8}$	$_{88}^{40}\mathrm{Zr}_{411}^{15}$	$_{108}^{41}\mathrm{Nb}_{502}^{18}$	$_{114}^{42}\mathrm{Mo}_{518}^{19}$	$_{123}^{43}\mathrm{Tc}_{550}^{20}$	$_{124}^{44}\mathrm{Ru}_{551}^{21}$	$_{108}^{45}\mathrm{Rh}_{479}^{18}$	$_{69}^{46}\mathrm{Pd}_{310}^{11}$	$_{37}^{47}\mathrm{Ag}_{177}^{6}$	$_{16}^{48}\mathrm{Cd}_{75}^{3}$	$_{39}^{49}\mathrm{In}_{181}^{7}$	$_{50}^{50}\mathrm{Sn}_{223}^{8}$	$_{46}^{51}\mathrm{Sb}_{202}^{8}$	$_{37}^{52}\mathrm{Te}_{164}^{6}$	$_{21}^{53}\mathrm{I}_{94}^{4}$	$_{0.8}^{54}\mathrm{Xe}_{4.4}^{0.1}$
$_{3}^{55}\mathrm{Cs}_{19}^{1}$	$_{11}^{56}\mathrm{Ba}_{58}^{2}$	$_{42}^{57}\mathrm{La}_{210}^{7}$	$_{72}^{72}\mathrm{Hf}_{351}^{12}$	$_{117}^{73}\mathrm{Ta}_{544}^{19}$	$_{145}^{74}\mathrm{W}_{658}^{24}$	$_{142}^{75}\mathrm{Re}_{639}^{24}$	$_{149}^{76}\mathrm{Os}_{668}^{25}$	$_{124}^{77}\mathrm{Ir}_{556}^{21}$	$_{100}^{78}\mathrm{Pt}_{453}^{17}$	$_{58}^{79}\mathrm{Au}_{238}^{8}$	$^{80}\mathrm{Hg}$	$_{26}^{81}\mathrm{Tl}_{122}^{4}$	$_{29}^{82}\mathrm{Pb}_{135}^{5}$	$_{31}^{83}\mathrm{Bi}_{145}^{5}$	$_{12}^{84}\mathrm{Po}_{63}^{2}$	$^{85}\mathrm{At}$	$_{0.9}^{86}\mathrm{Rn}_{5.2}^{0.2}$
$^{87}\mathrm{Fr}$	$^{88}\mathrm{Ra}$	$^{89}\mathrm{Ac}$															

$_{48}^{58}\mathrm{Ce}_{236}^{8}$	$_{39}^{59}\mathrm{Pr}_{193}^{7}$	$_{34}^{60}\mathrm{Nd}_{168}^{6}$	$^{61}\mathrm{Pm}$	$_{21}^{62}\mathrm{Sm}_{103}^{3}$	$_{13}^{63}\mathrm{Eu}_{67}^{2}$	$_{45}^{64}\mathrm{Gd}_{218}^{7}$	$_{46}^{65}\mathrm{Tb}_{223}^{8}$	$_{35}^{66}\mathrm{Dy}_{168}^{6}$	$_{34}^{67}\mathrm{Ho}_{166}^{6}$	$_{38}^{68}\mathrm{Er}_{185}^{6}$	$_{31}^{69}\mathrm{Tm}_{148}^{5}$	$_{15}^{70}\mathrm{Yb}_{74}^{2}$	$_{53}^{71}\mathrm{Lu}_{252}^{9}$
$_{59}^{90}\mathrm{Th}_{294}^{10}$	$^{91}\mathrm{Pa}$	$_{85}^{92}\mathrm{U}_{340}^{14}$	$^{93}\mathrm{Np}$	$^{94}\mathrm{Np}$	$^{95}\mathrm{Am}$	$^{96}\mathrm{Cm}$	$^{97}\mathrm{Bk}$	$^{98}\mathrm{Cf}$	$^{99}\mathrm{Es}$	$^{100}\mathrm{Fm}$	$^{101}\mathrm{Md}$	$^{102}\mathrm{No}$	$^{103}\mathrm{Lw}$

Based on:

$G_C \approx \dfrac{W_C}{6a^2}$	$\Psi_C \approx \dfrac{G_C}{a}$	$\nu \approx 0$	$E \approx \dfrac{27}{2}\Psi_C$	$\sigma_C \approx \dfrac{E}{6}$	$\tau_C \approx \dfrac{E}{4\pi}$	$\varepsilon_C \approx \dfrac{2}{3}$	$\gamma_C \approx \mathrm{atan}\,\dfrac{1}{2}$

ν = Poisson's ratio (material-independent), E = Young's modulus, σ_C = critical normal stress, τ_C = critical shear stress, ε_C = critical normal strain (material-independent), γ_C = critical shear strain (material-independent), G_C = fracture energy (per unit area), Ψ_C = fragmentation energy (per unit volume), $K_{IC} = \sqrt{G_C E}$ = fracture toughness, W_C = cohesion energy, a = interatomic distance, Z = atomic number – (material properties referred to 0 K).

Source: Pugno, N. et al., *Int. J. Solids Struct.*, 43, 5647–5657, 2006. With permission.

to confirm the observation of the ideal strength. Our model agrees with such a prediction for carbon.

The membranes were analyzed by scanning tunneling microscopy (STM), confirming the absence of defects over an area of hundreds of square nanometers, a size comparable to that of the highly stressed zone developed under the nanoindenter tip. Since the stress–concentration rapidly decays by increasing the distance from the point where the load is applied, moderate defects placed far from the contact zone could not prevail, as observed. However, defects are thermodynamically unavoidable. At the thermal equilibrium, the vacancy fraction, $f = n/N$, where n is the number of vacancies and N is the total number of atoms, is estimated to be $f \approx e^{-W_C/(k_B T)}$, where $W_C \approx 7\,\text{eV}$ is the energy to remove one carbon atom and T is the absolute temperature at which the carbon is assembled. Considering a maximum value of $T \approx 4000\,\text{K}$ leads to $f \approx 1.5 \times 10^{-9}$, thus to a maximum number $N \approx 6.5 \times 10^8$ of atoms in which less than one vacancy is expected (Pugno, 2007). This corresponds to a defect-free maximum surface area of the order of one square micrometer, thus again compatible with the observation. Even if atomistic defects are tediously and not easily observable by STM investigation and the defect density is usually imposed by the fabrication process rather than by the thermodynamic limit, our model agrees with the observations.

23.11 Model Limitations

The values that we have reported in the "preliminary periodic table for the nanomechanical properties of elements" (Table 23.1) are affected by different uncertainties.

In particular, we have simply assumed the Poisson's ratio equal to zero, as suggested by the considerations reported in Section 23.5; however, zero represents an intermediate value between its thermodynamic limits of −1 and 1/2. Furthermore, we have to note that the Poisson's ratio is an anisotropic parameter, depending on the crystallographic direction along which it is measured: thus, different values should be considered for each different crystallographic direction. For the sake of simplicity, to present a preliminary periodic table, we have chosen to ignore anisotropy. Note that the classical periodic table of the elements itself ignores anisotropy, reporting mean values, as for example for the electrical or thermal conductivity, as well as for the atomic radius. The "atomic radius" itself has a degree of uncertainty, which affects our predictions. In fact, different types of atomic radii can be defined through different models, e.g., Hartree–Fock approach, rigid spheres, and so on. A few of them are reported in the periodic table of elements in terms of atomic (or also covalent or ionic) radius or volume. We note that the atomic radius and volume are independent parameters, thus representing a first reason of uncertainty. In addition, as previously emphasized, we have neglected anisotropy. However, in our approach, different values for each crystallographic direction of the parameter a could allow us to roughly take into account anisotropy, as well as a "mean value" (e.g., the cubic root of the volume per atom) would allow us to consider not only simple cubic lattice. Finally, our model ignores plastic deformations.

To clarify the previous points, we can treat as a simple example the case of sodium, considering its lattice parameter (BCC, 0.42906 nm) and applying the rigid sphere model (two atoms per cell in BCC). Young's modulus of sodium usually reported in the literature is close to 10 GPa, against our preliminary prediction of 14 GPa. According to the periodic table of the elements, the atomic radius of the sodium (that we have used) is 0.190 nm, whereas the atomic radius that we calculate, remembering that the closed packed direction is [111] (diagonal), is 0.186 nm. The same value is deduced starting from the volume of the unit cell (cube of the lattice parameter for BCC) and taking into account the packing factor for BCC (0.68). Thus, considering 0.186 nm instead of 0.190 nm would yield $E \approx 14 \cdot 0.190^3/0.186^3 \approx 15\,\text{GPa}$. On the other hand, removing the approximation of a vanishing Poisson's ratio, $E/(1 - 2\nu) \approx 15\,\text{GPa}$, so that to capture the correct value of $E \approx 10\,\text{GPa}$, a value of $\nu \approx 0.17$ is deduced.

23.12 Conclusions

We conclude that our model must be considered a basic treatment; however, in spite of its limits, the approach reported in this chapter could be of interest due to its simplicity and generality for estimating the nanomechanical properties of the elements.

References

Berger, C., Song, Z., Li, X., Wu, X., Brown, N., Naud, C., Mayou, D. et al., 2006, Electronic confinement and coherence in patterned epitaxial graphene, *Science* 312, 1191–1196.

Carpinteri, A., 1997, *Structural Mechanics—A Unified Approach*, E & FN Spon, New York.

Carpinteri, A. and Pugno, N., 2002, One-, two- and three-dimensional universal laws for fragmentation due to impact and explosion, *J. Appl. Mech.* 69, 854–856.

Carpinteri, A. and Pugno, N., 2004, Scale-effects on average and standard deviation of the mechanical properties of condensed matter: An energy based unified approach, *Int. J. Fract.* 128, 253–261.

Casari, C. S., Li Bassi, A., and Bottani, C. E., 2001, Acoustic phonon propagation and elastic properties of cluster-assembled carbon films investigated by Brillouin light scattering, *Phys. Rev. B* 64, 85417-1–85417-5.

Chopra, N. G., Luyken, R. J., Cherrey, K., Crespi, V. H., Cohen, M. L., Louie, S. G., and Zettl, A., 1995, Boron nitride nanotubes, *Science* 269, 966–968.

Dikin, D. A., Stankovich, S., Zimney, E. J., Piner, R. D., Dommett, G., Evmenenko, S., Nguyen, T. et al., 2007, Preparation and characterization of graphene oxide paper, *Nature* 448, 457–460.

Frenkel, J. Z., 1926, Zur theorie der elastizit. atsgrenze und der festigkeit kristallinischer körper, *Z. für Phys.* 37, 572–609.

Iijima, S., 1991, Helical microtubules of graphitic carbon, *Nature* 354, 56–58.

Jiang, H., Liu, B., Huang, Y., and Hwang, K. C., 2004, Thermal expansion of single wall carbon nanotubes, *J. Eng. Mater. Technol.* 126, 265–270.

Kittel, C., 1966, *Introduction to Solid State Physics,* John Wiley & Sons, New York.

Lambin, P. H., Meunier, V., and Biró, L. P., 1998, Elastic deformation of a carbon nanotube adsorbed on a stepped surface, *Carbon* 36, 701–704.

Lee, C., Wei, X., Kysar, J. W., and Hone, J., 2008, Measurement of the elastic properties and intrinsic strength of monolayer graphene, *Science* 321, 385–388.

Loiseau, A., Willaime, F., Demoncy, H., Hug, G., and Pascard, H., 1996, Boron nitride nanotubes with reduced numbers of layers synthesized by arc discharge, *Phys. Rev. Lett.* 76, 4737–4740.

Macmillan, N. H., 1983, The ideal strength of solids, in: R. Latanision and J.R. Pickens (eds.), *Atomistics of Fracture*, Plenum Press, New York, pp. 95–164.

Novoselov, K. S., Geim, A. K., Morozov, S. V., Jiang, D., Zhang, Y., Dubonos, S. V., Grigorieva, I. V. et al., 2004, Electric field effect in atomically thin carbon films, *Science* 306, 666–669.

Orowan, E., 1948, Fracture and strength of solids, *Rep. Prog. Phys.* XII, 185–232.

Pugno, N., 2007, The role of defects in the design of the space elevator cable: From nanotube to megatube, *Acta Mater.* 55, 5269–5279.

Pugno, N., 2008, A journey on the nanotube, in the top ten advances in materials, *Mater. Today* 11, 40–45.

Pugno, N. and Carpinteri, A., 2003, Tubular adhesive joints under axial load, *J. Appl. Mech.* 70, 832–839.

Pugno, N. and Ruoff, R., 2004, Quantized fracture mechanics, *Philos. Mag.* 84, 2829–2845.

Pugno, N., Marino, F., and Carpinteri, A., 2006, Towards a periodic table for the nanomechanical properties of elements, *Int. J. Solids Struct.* 43, 5647–5657.

Qian, D., Wagner, G. J., Liu, W. K., Yu, M.-F., and Ruoff, R. S., 2002, Mechanics of carbon nanotubes, *Appl. Mech. Rev.* 55, 495–532.

Ross, P. E., 1991, Buckytubes: Fullerenes may form the finest, toughest fibers yet, *Sci. Am.* 265, 24–25.

Slater, J. C., 1940, Note on Grüneisen's constant for the incompressible metals, *Phys. Rev.* 57, 744–746.

Stankovich, S., Dikin, D. A., Dommett, G. H. B., Kohlhaas, K. M., Zimney, E. J., Stach, E. A., Piner, R. D. et al., 2006, Graphene-based composite materials, *Nature* 442, 282–285.

Treacy, M. M., Ebbesen, T. W., and Gibson, J. M., 1996, Exceptionally high Young's modulus observed for individual carbon nanotubes, *Nature* 381, 678–680.

Weng-Sieh, Z., Cherrey, K., Chopra, N. G., Blase, X., Yoshiyuki Miyamoto., Angel Rubio., Cohen, M. L. et al., 1995, Synthesis of $B_xC_yN_z$ nanotubules, *Phys. Rev. B* 51, 11229–11232.

Yakobson, B. I. and Smalley, R. E., 1997, Fullerene nanotubes: C-1000000 and beyond, *Am. Sci.* 85, 324–337.

Yakobson, B. I., Brabec, C. J., and Bernholc, J., 1996, Nanomechanics of carbon nanotubes: Instabilities beyond linear response, *Phys. Rev. Lett.* 76, 2511–2514.

Yakobson, B. I., Campbell, M. P., Brabec, C. J., and Bernholc, J., 1997, High strain rate fracture and C-chain unraveling in carbon nanotubes, *Comput. Mater. Sci.* 8, 341–348.

Yu, M.-F., Lourie, O., Dyer, M. J., Moloni, K., Kelly, T. F., and Ruoff, R. S., 2000, Strength and breaking mechanism of multiwalled carbon nanotubes under tensile load, *Science* 287, 637–640.

Zhang, P., Huang, Y., Geubelle, P. H., Klein, P. A., and Hwang K. C., 2002, The elastic modulus of single-wall carbon nanotubes: A continuum analysis incorporating interatomic potentials, *Int. J. Solids Struct.* 39, 3893–3906.